

KDM2B promotes pancreatic cancer via Polycomb-dependent and -independent transcriptional programs

Alexandros Tzatsos,^{1,2} Polina Paskaleva,¹ Francesco Ferrari,³ Vikram Deshpande,⁴ Svetlana Stoykova,¹ Gianmarco Contino,¹ Kwok-Kin Wong,^{2,5} Fei Lan,⁶ Patrick Trojer,⁶ Peter J. Park,³ and Nabeel Bardeesy^{1,2}

¹Massachusetts General Hospital Cancer Center, Boston, Massachusetts, USA. ²Department of Medicine and ³Center for Biomedical Informatics, Harvard Medical School, Boston, Massachusetts, USA. ⁴Department of Pathology, Massachusetts General Hospital and Harvard Medical School, Boston, Massachusetts, USA. ⁵Department of Medical Oncology, Dana-Farber/Harvard Cancer Center, Boston, Massachusetts, USA. ⁶Constellation Pharmaceuticals, Cambridge, Massachusetts, USA.

Epigenetic mechanisms mediate heritable control of cell identity in normal cells and cancer. We sought to identify epigenetic regulators driving the pathogenesis of pancreatic ductal adenocarcinoma (PDAC), one of the most lethal human cancers. We found that KDM2B (also known as Ndy1, FBXL10, and JHDM1B), an H3K36 histone demethylase implicated in bypass of cellular senescence and somatic cell reprogramming, is markedly overexpressed in human PDAC, with levels increasing with disease grade and stage, and highest expression in metastases. KDM2B silencing abrogated tumorigenicity of PDAC cell lines exhibiting loss of epithelial differentiation, whereas KDM2B overexpression cooperated with *Kras*^{G12D} to promote PDAC formation in mouse models. Gain- and loss-of-function experiments coupled to genome-wide gene expression and ChIP studies revealed that KDM2B drives tumorigenicity through 2 different transcriptional mechanisms. KDM2B repressed developmental genes through cobinding with Polycomb group (PcG) proteins at transcriptional start sites, whereas it activated a module of metabolic genes, including mediators of protein synthesis and mitochondrial function, cobound by the MYC oncogene and the histone demethylase KDM5A. These results defined epigenetic programs through which KDM2B subverts cellular differentiation and drives the pathogenesis of an aggressive subset of PDAC.

Introduction

Pancreatic ductal adenocarcinoma (PDAC) is the most common type of pancreatic malignancy and has a poor prognosis, with most patients dying within the first year of diagnosis (1). The spectrum of genetic lesions in PDAC includes highly recurrent activating KRAS mutations and loss of function of the *CDKN2A*, *TP53*, and *SMAD4* tumor suppressors (2). However, readily “druggable” molecular targets have not yet been identified in this cancer. Global gene expression analysis and functional studies have defined a subtype of PDAC (termed quasimesenchymal) showing particularly poor outcomes and chemoresistance, characterized by a gene signature consistent with partial loss of epithelial differentiation and acquisition of mesenchymal features (3, 4). Thus, there is an immediate need to identify new targets for the treatment of PDAC in general, and this aggressive subtype in particular.

Epigenetic mechanisms are central to the initiation and progression of cancers, and the biochemical mediators of these processes could serve as new, more efficacious therapeutic targets (5, 6). In this regard, recurrent genetic alterations and changes in expression of chromatin regulators have been identified in many human tumors (6). Altered activity of histone demethylases (HDMs) is emerging as a common defect (7), with loss-of-

function mutations in the H3K27 demethylase *KDM6A* (also known as *UTX*) suggesting tumor suppressor functions (8), and amplification or overexpression of the H3K9/H3K36 demethylase *KDM4C* consistent with positive roles in tumorigenesis (9). Recent studies have demonstrated that the H3K36me2 demethylase KDM2B is also an important regulator of cell growth (10–14). KDM2B promotes bypass of senescence in primary cells, in part by suppressing the *CDKN2A* tumor suppressor locus through direct binding and histone demethylation, which leads to recruitment of the Polycomb repressive complex II (PRC2) (12, 13). KDM2B is preferentially expressed in ES cells and is required for the reprogramming of somatic cells toward a pluripotent state, linking this HDM to suppression of differentiation (15). In keeping with a cancer-relevant role, KDM2B promotes leukemia development in mouse models (16) and enhances migration and angiogenic activity of human bladder cancer cell lines in vitro via induction of the PRC2 component EZH2 (11). However, the contribution of KDM2B to the progression and maintenance of epithelial cancers remains to be fully elucidated. Furthermore, whereas KDM2B has an established role as an H3K36me2 demethylase repressing selected target genes, the global transcriptional functions and genome-wide targets of KDM2B are unknown.

In the present study, we investigated whether dysregulated HDM family members induce epigenetic reprogramming in PDAC and contribute to PDAC pathogenesis. We identified KDM2B as a major mediator driving the tumorigenicity of poorly differentiated PDAC through 2 complementary but distinct tran-

Authorship note: Polina Paskaleva and Francesco Ferrari contributed equally to this work.

Conflict of interest: Fei Lan and Patrick Trojer are employees of Constellation Pharmaceuticals Inc.

Citation for this article: *J Clin Invest.* 2013;123(2):727–739. doi:10.1172/JCI64535.

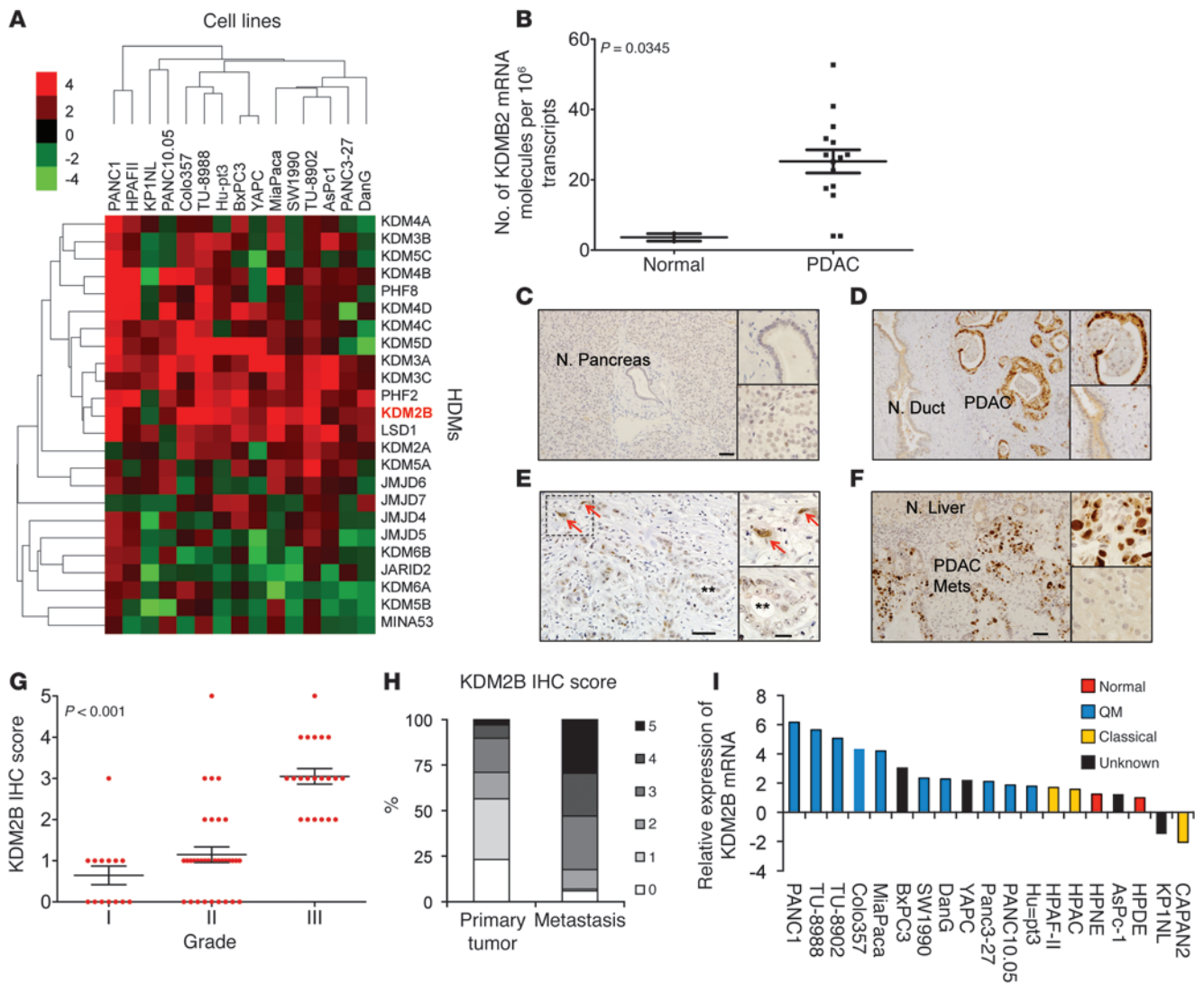


Figure 1
 KDM2B is upregulated in advanced PDAC. (A) Heat map of quantitative RT-PCR data showing relative expression of HDM family members in human PDAC cell lines versus HPDE cells. Color bar indicates relative fold change. (B) KDM2B transcript levels in a series of human PDAC specimens compared with normal pancreatic tissue, determined by RNA-seq (samples from MGH tumor bank). (C–F) IHC staining for KDM2B in human pancreatic tissues. (C) Normal (N.) adult pancreas was negative for KDM2B. Insets: higher magnification of normal duct and islet. (D) PDAC showing strong nuclear expression in neoplastic cells, whereas normal duct cells were negative. Insets: higher magnification of PDAC cells (top) and normal duct (bottom). (E) Primary PDAC showing stronger staining of the poorly differentiated component (arrows) compared with the well-differentiated glandular component (asterisks). Insets: Higher magnification of poorly differentiated (top) and glandular (bottom) elements. (F) PDAC liver metastasis showed strong staining of tumor cells, whereas normal liver parenchyma was negative. Inset: higher magnification of PDAC cells (top) and normal liver (bottom). Scale bars: 50 μ m; 20 μ m (insets). (G) Relative KDM2B IHC staining score for 69 primary PDAC specimens of different grades. (H) Percent distribution of KDM2B staining scores in primary and metastatic tumors. (I) Quantitative RT-PCR analysis of relative KDM2B expression in PDAC cell lines versus HPDE and HPNE cells. Cell lines were classified as quasimesenchymal (QM) and classical based on ref. 4. See also Supplemental Figure 1.

scriptional programs. Functional interactions with Polycomb group (PcG) complexes overrode cell fate decisions, whereas with interplay, MYC and KDM5A sustained metabolic gene expression. KDM2B bound transcriptional start sites (TSSs) in discrete modules with these transcriptional regulators, leading to either stable repression or activation of gene expression. Thus, our results provide insights into the epigenetic machinery in PDAC and suggest therapeutic strategies for a highly aggressive and clinically intractable subtype of this malignancy.

Results

KDM2B is upregulated and associated with advanced disease in PDAC. We sought to identify HDMs that are overexpressed in PDAC and are potential novel regulators of PDAC pathogenesis. Quantitative real-time PCR analysis revealed that HDMs as a group were broadly dysregulated in PDAC cell lines compared with immortal, but not transformed, human pancreatic ductal epithelial (HPDE) and human pancreatic nestin-expressing (HPNE) cells (Figure 1A). Furthermore, bioinformatics analysis of SAGE datasets of micro-



Table 1
Expression of HDMs in human PDAC specimens

HDM	Normal ducts	PDAC specimens
<i>KDM2B</i>	0	21 ± 11
<i>KDM5A</i>	0	29 ± 20
<i>KDM6B</i>	0	21 ± 13
<i>KDM3C</i>	0	24 ± 14

Meta-analysis of SAGE data (presented as mean ± SD number of sequenced tags) comparing overexpressed HDMs in human PDAC specimens and microdissected normal pancreatic ductal cells. Data are from ref. 2.

dissected normal human pancreatic ducts and human PDAC specimens showed that of approximately 30 predicted HDMs, 4 (*KDM2B*, *KDM5A*, *KDM6B*, and *KDM3C*) were absent in normal ductal epithelium and showed robust upregulation in PDAC tissue (Table 1). Among these highly upregulated HDMs, the H3K36 demethylase *KDM2B* has been implicated in bypass of cellular senescence, induction of pluripotency, and tumorigenesis and was selected for further characterization in PDAC.

First, we confirmed that *KDM2B* was overexpressed in an additional set of human PDAC specimens (Figure 1B). To support these mRNA expression data, we analyzed *KDM2B* protein expression in vivo via immunohistochemistry (IHC) in 69 sequential cases of resected human PDAC and 17 liver metastasis specimens (for antibody characterization, see Supplemental Figure 1, A and B; supplemental material available online with this article; doi:10.1172/JCI64535DS1). Whereas normal adult pancreas was completely negative for *KDM2B* (Figure 1C), the majority of PDAC specimens had nuclear expression of *KDM2B*, specifically in the neoplastic epithelium (Figure 1, D–F), with varying degrees of staining both within and between tumors. Quantification of the staining scores in PDAC (see Methods) revealed a strong association between abundance of *KDM2B*-positive cells and higher tumor grade ($P < 0.001$; Figure 1G). Moreover, even in lower-grade tumors that were mainly *KDM2B*-negative, *KDM2B* expression was typically highly enriched in the poorly differentiated, invasive cells detached from the glandular structures (Figure 1E). In addition, metastases showed the highest relative staining for *KDM2B*, with 9 of 17 metastases having staining scores of 4 and 5, compared with 7 of 69 nonmetastatic tumors ($P < 0.00001$; Figure 1, F and H). Comparable staining profiles were seen with a second *KDM2B* antibody (Supplemental Figure 1A). As predicted by the mRNA expression analysis (Figure 1A), we found that *KDM2B* protein was upregulated in human PDAC cell lines compared with HPDE and HPNE cells (Supplemental Figure 1C). Notably, the expression profile of *KDM2B* in higher-grade PDAC was recapitulated in vitro, as we observed preferential *KDM2B* expression in poorly differentiated (quasimesenchymal) PDAC cell lines, which exhibit a poor prognosis mesenchymal gene signature (3, 4), compared with well-differentiated (classical) PDAC cells, which express epithelial and adhesion-associated genes (Figure 1I). Collectively, these data revealed that *KDM2B* is upregulated in PDAC, with highest levels specifically associated with advanced disease and a poorly differentiated state.

KDM2B is required for tumorigenicity of poorly differentiated PDAC cancer cell lines. We used human PDAC cell lines to evaluate the potential functional roles of *KDM2B* in this cancer. We tested 2 different short hairpins that efficiently knock down *KDM2B*

(Supplemental Figure 2A) in selected PDAC cell lines exhibiting high levels of *KDM2B* expression (MiaPaca, PANC1, TU-8988, and LZ10.7 cells). We found that knockdown of *KDM2B* dramatically attenuated cell proliferation, led to sharp reductions in anchorage-independent growth, and effectively blocked xenograft tumor formation in each of these cell lines (Figure 2, A and B, and data not shown), suggestive of a requirement for *KDM2B* in tumor growth. There was no evidence for apoptosis, whereas some cell lines (e.g., LZ10.7) adopted a senescence-like appearance (Supplemental Figure 2B). Importantly, the proliferative arrest, senescence response, and tumorigenicity in vivo were rescued by concurrent overexpression of a nontargeted wild-type *KDM2B* construct, but not by a Jumonji C (JmjC) domain deletion mutant (Figure 2C and Supplemental Figure 2, B and C), demonstrating the specificity of the hairpins and the requirement for the *KDM2B* JmjC domain for PDAC growth in vitro and in vivo. Moreover, *KDM2B* knockdown did not significantly affect the proliferation of HPDE cells (Supplemental Figure 2D), further demonstrating the specificity of these studies.

Examination of a larger panel of PDAC cell lines ($n = 14$ cell lines) revealed that the quasimesenchymal subset had a substantially higher sensitivity to *KDM2B* knockdown than did the classical subset (Figure 2D), consistent with the preferential overexpression of *KDM2B* in these poorly differentiated cell lines (Figure 1G). Thus, *KDM2B* is required for tumorigenicity of PDAC cell lines, and, in keeping with its upregulation in advanced tumors in vivo, is particularly important in cell lines that exhibit loss of epithelial differentiation. Several of the *KDM2B*-dependent cell lines harbor homozygous deletion of the *CDKN2A* locus (e.g., MiaPaca, YAPC, and TU-8988), which indicates that function of *KDM2B* in PDAC extends beyond its capacity to repress this locus.

KDM2B cooperates with *Kras*^{G12D} to drive PDAC development in mouse models. We next sought to assess whether forced *KDM2B* expression could directly drive the development of PDAC in vivo. In both humans and mice, activated *Kras*^{G12D} initiates the formation of focal premalignant ductal lesions, termed pancreatic intraepithelial neoplasias (PanINs), which progress to PDAC upon inactivation of either *CDKN2A* or *TP53* (17–19). To examine the effect of *KDM2B* on PDAC progression, we took advantage of a transplantable model system of multistage tumorigenesis (20) that uses primary mouse pancreatic ductal cells expressing endogenous levels of *Kras*^{G12D} and in which *Cdkn2a* and *Tp53* are intact (*Ptf1α-Cre;LSL-Kras*^{G12D} cells; Figure 2E). We found that overexpression of *KDM2B* enhanced in vitro proliferation of these cells, whereas a dominant-negative *KDM2B* mutant (10, 12, 13) lacking the JmjC domain suppressed proliferation (Figure 2F). Orthotopic injection of *Kras*^{G12D} control cells produced no lesions (Table 2 and Figure 2G), or focal PanIN when increased cell numbers were used (Supplemental Figure 2E). In contrast, overexpression of wild-type *KDM2B* resulted in development of invasive PDAC (5 of 5 mice) upon injection of only 20,000 cells (Table 2 and Figure 2G). Histological examination revealed that these tumors consisted mainly of poorly differentiated elements (Figure 2G, right, inset). Moreover, as in human PDAC cell lines, *Kdm2b* was upregulated in PDAC cell lines derived from the *Pdx1-Cre;LSL-Kras*^{G12D}; *p53*^{Lox/+} mouse model (21) compared with nontransformed ductal cells (Supplemental Figure 2F), and shRNA-mediated *Kdm2b* knockdown strongly impaired proliferation and tumorigenicity of these mouse PDAC lines (Supplemental Figure 2G). Thus, *KDM2B* is critical for tumor

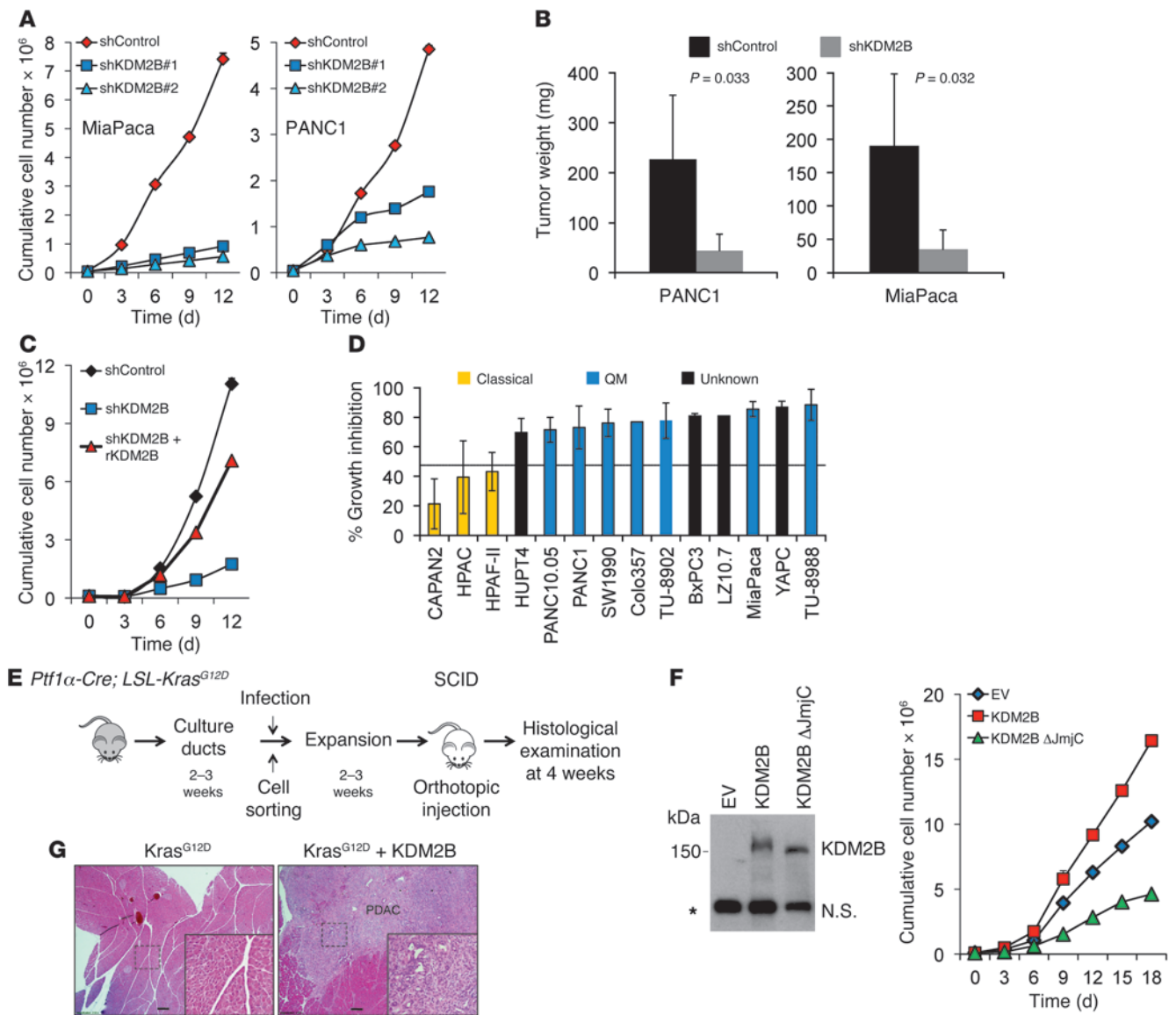


Figure 2 KDM2B is required for tumorigenicity of poorly differentiated PDAC cell lines. (A and B) Human PDAC cell lines (MiaPaca and PANC1) were infected with lentiviruses expressing empty vector (shControl) or 2 different shRNAs against KDM2B (shKDM2B) and assessed by (A) in vitro growth assays and (B) subcutaneous tumorigenesis (xenograft) experiments (see Methods). (C) Growth curve showing that overexpression of a nontargeted wild-type KDM2B construct (rKDM2B) rescued the proliferative arrest induced by shKDM2B. (D) Percent growth inhibition of a panel of PDAC cell lines upon knockdown of KDM2B (9 days after seeding). Results are mean \pm SD. (E–G) Transplantable murine PanIN-PDAC progression model using *Ptf1 α -Cre; LSL-Kras^{G12D}* pancreatic ductal cells. Cells were transduced with lentiviruses to overexpress wild-type and JmjC domain deletion mutant (Δ JmjC) of KDM2B. EV, empty vector. (E) Schematic of model system. (F) Western blot of KDM2B expression in transduced ductal cells and in vitro growth curves. Asterisk denotes nonspecific (N.S.) band. (G) Histological images of the pancreas 4 weeks after orthotopic injection with 2×10^4 cells. Control *Kras^{G12D}* cells failed to form tumors, whereas wild-type KDM2B induced poorly differentiated PDAC. Insets show high-magnification views of the boxed regions (enlarged $\times 4$). Scale bars: 200 μ m. See also Supplemental Figure 2.

maintenance in both mouse and human PDAC and cooperates with *Kras^{G12D}* in primary mouse ductal cells to drive the formation of poorly differentiated tumors in vivo.

KDM2B is required for Polycomb-mediated repression and for maintenance of a metabolic gene signature. To begin to explore at the molecular level how KDM2B exerts its oncogenic effects in PDAC, we undertook an unbiased genomic approach to define the transcriptional program controlled by KDM2B. We performed digital

expression profiling analysis (direct RNA sequencing) to identify transcripts differentially expressed upon KDM2B knockdown in 6 human PDAC cell lines that showed strong responsiveness to KDM2B knockdown (Figure 2D). Strikingly, Gene Set Enrichment Analysis (GSEA) of differentially expressed genes revealed that knockdown of KDM2B caused consistent alterations in 2 major gene expression modules (Figure 3A). The upregulated genes closely matched a set of genes that are repressed by PRC2



Table 2
Transplantable murine PanIN-PDAC progression model using *Ptf1α-Cre;LSL-Kras^{G12D}* pancreatic ductal cells

Type of injection	PDAC incidence
Empty vector	0/5
KDM2B	5/5
KDM2B JmjC deletion mutant	0/3

Cells were transduced with lentiviruses to overexpress wild-type and JmjC domain deletion mutant of KDM2B. Shown is the incidence of PDAC upon orthotopic injection.

components in ES cells and prostate cancer cell lines (22, 23), consistent with a requirement of KDM2B for PRC2-dependent transcriptional repression. The second module, consisting of genes downregulated upon KDM2B inactivation, was enriched for genes involved in ribosomal biogenesis, mRNA processing, and translation (Figure 3A), which suggests that KDM2B may either directly or indirectly maintain expression of key regulators of metabolic homeostasis.

The findings from GSEA were extended by *in silico* prediction of transcription factor networks using Ingenuity Pathway Analysis (IPA) software. IPA indicated that KDM2B knockdown resulted in the activation of transcriptional programs known to be antagonized by PRC2, including SMARCA4 (also known as BRG1/BAF190) and SMARCB1 (also known as SNF5 and BAF471), which are components of the SWI/SNF chromatin remodeling complex and established PDAC tumor suppressors (24, 25), and HOXD3 (Figure 3B). Interestingly, this analysis also revealed the downregulation of transcriptional programs driven by MYC family transcription factors (Figure 3B), which are established oncogenes that drive metabolic reprogramming of cancer cells. Consistent with direct roles of KDM2B in the regulation of these pathways, KDM2B overexpression in primary mouse *Kras^{G12D}*-expressing pancreatic ductal cells induced a MYC transcriptional signature (Supplemental Figure 3A) and concomitantly repressed TP53 and PcG targets, as determined by RNA sequencing (RNA-seq) profiling (Supplemental Figure 3, A and B). The suggested functions of both MYC and PRC2 in the KDM2B transcriptome are notable in light of the known roles of these factors in driving progression of poorly differentiated cancers (26–30).

Next, we examined whether expression changes in PRC2 components or MYC could account for the observed alterations in expression of their respective target genes. Knockdown of KDM2B downregulated the mRNA and protein levels of EZH2 in a subset of cell lines (e.g., MiaPaca and SW1990; Supplemental Figure 3, C and D), in line with previous observations (11–13). However, a similar profile of Polycomb-related genome-wide expression changes was observed even in cell lines in which knockdown did not affect total EZH2 levels (e.g., TU-8988 and TU-8902; Supplemental Figure 3, C and D), which suggests that KDM2B may also facilitate recruitment of PRC2 to target loci or enhance its methyltransferase activity (11, 12). In contrast, MYC expression was not strongly altered by KDM2B knockdown (Supplemental Figure 3E), whereas all PDAC cell lines showed reduced KDM5A expression (Figure 3, C and D). This H3K4 trimethyl-demethylase, which was highly overexpressed in our PDAC specimens (Figure 1B), is implicated in metabolic homeostasis and cancer and genetically interacts with both *d-Myc* and *dKDM2* to regulate growth

decisions in *Drosophila* (31–35). These considerations suggested a potential role of KDM5A and its interplay with MYC in the KDM2B transcriptional program.

Distinct modular associations of KDM2B at transcriptionally repressed and activated targets. Recent large-scale ChIP studies have indicated that epigenetic regulators may be organized into modules that independently cobind common target genes, characterized by shared chromatin states and related physiological functions without necessarily forming physical complexes (35). To identify direct transcriptional targets of KDM2B and discover its potential functional interactions, we mapped the genome-wide binding sites of KDM2B, EZH2, and KDM5A in PANC1 cells by ChIP followed by DNA sequencing (ChIP-seq; see Supplemental Figure 4, A and B, and Methods for KDM2B antibody validation). Peak detection analysis revealed that comparable numbers of target loci were bound by KDM2B, EZH2, and KDM5A (3,237, 2,118, and 3,504 sites, respectively). The set of EZH2 and KDM5A targets showed considerable similarity to those reported in other cell types (Supplemental Figure 4C), which suggests that these binding patterns are largely conserved. We observed striking overlaps in the binding profiles of the different factors. Indeed, KDM2B cobound 31% of the EZH2 targets and 25% of the KDM5A targets, whereas there was virtually no overlap in the binding of EZH2 with KDM5A (Figure 4A). Comparison of these data with published MYC binding profiles (from ES and HeLa cells) indicated that there was also prominent binding overlap of MYC with KDM2B and/or KDM5A, but not with EZH2 (Figure 4, B and C). The overlap of KDM2B and KDM5A-MYC was unexpected and suggested that KDM2B cooperates with these proteins at target loci in addition to sustaining KDM5A mRNA expression.

IPA indicated that the KDM2B binding modules were associated with coherent gene sets (Figure 4, D and E). In particular, KDM2B-EZH2-cobound genes are involved in developmental and pluripotency networks, whereas genes bound by KDM2B together with KDM5A and/or MYC participate in metabolic processes, including regulation of protein synthesis through the eukaryotic initiation factor 2 (EIF2) and mammalian target of rapamycin (mTOR) pathways, and energy homeostasis through control of oxidative phosphorylation and mitochondrial function (Figure 4, D and E, and Supplemental Figure 4D). Notably, these patterns are reminiscent of the KDM2B transcriptome in PDAC cell lines (Figure 3A). Collectively, the data suggest that KDM2B regulates at least 2 independent transcriptional programs by cobinding to target genes with either EZH2 or KDM5A-MYC, as well as by indirectly controlling expression levels of EZH2 and KDM5A.

Fine-scale analysis of chromatin binding showed that KDM2B and EZH2 formed bimodal peaks that surrounded the TSSs, whereas KDM5A formed sharp peaks over the TSS (Figure 5A); interestingly, the binding pattern of KDM2B was shifted depending on the presence of either EZH2 or KDM5A (Supplemental Figure 5A). Each of these factors was preferentially bound to CpG-rich promoters (Figure 5B). Moreover, meta-analysis of the DNA methylation pattern in PANC1 cells revealed the promoters bound by KDM2B alone or in the context of KDM5A were unmethylated, whereas those bound by KDM2B-EZH2 were methylated, regardless of the presence of CpG islands (Figure 5C).

Notably, stratification of gene expression and genome-wide pairwise comparison of KDM2B binding with H3K4me3 enrichment in PANC1 cells demonstrated that KDM2B bound both active and inactive promoters (Figure 5D and Supplemental Figure 5B). In

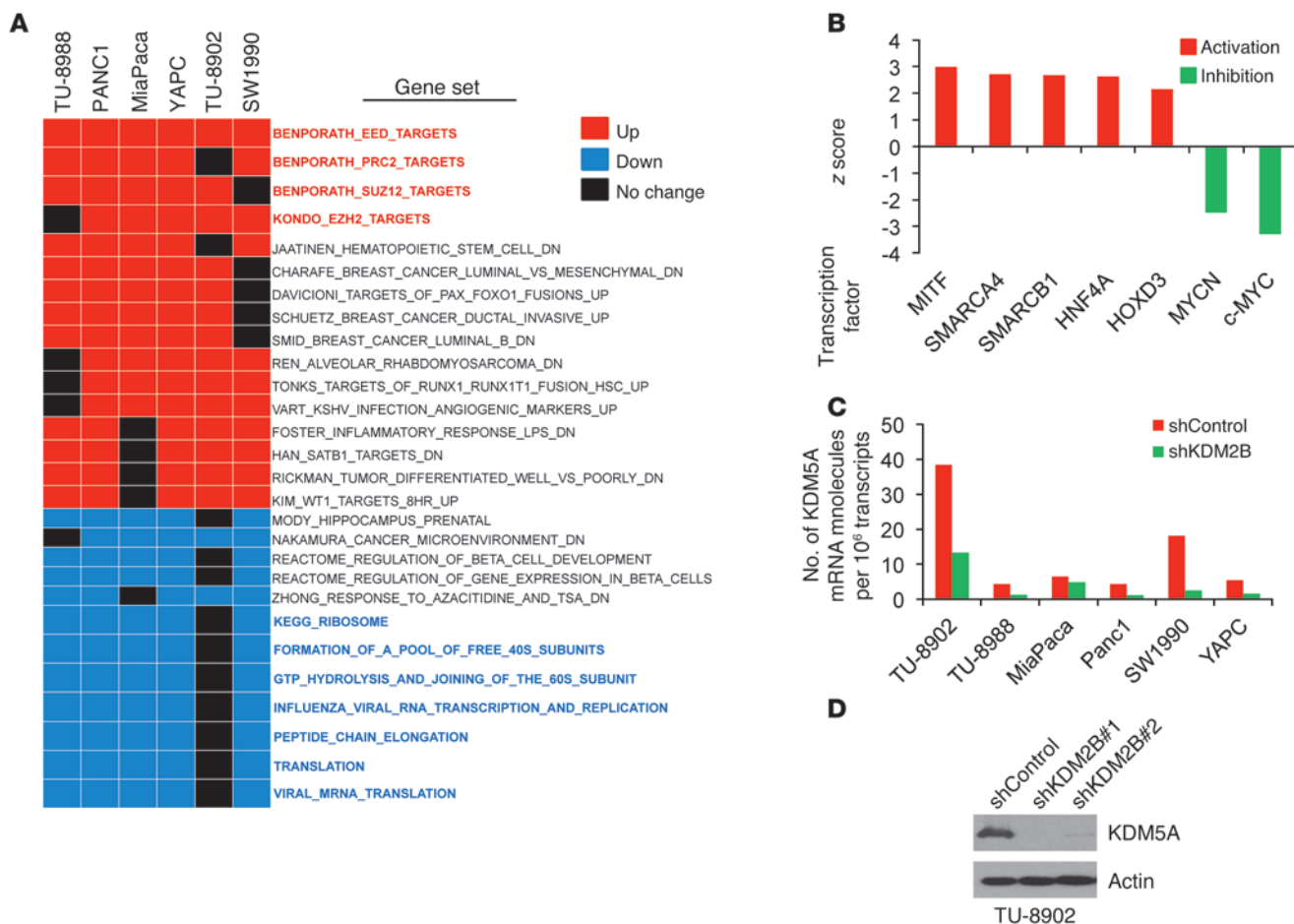
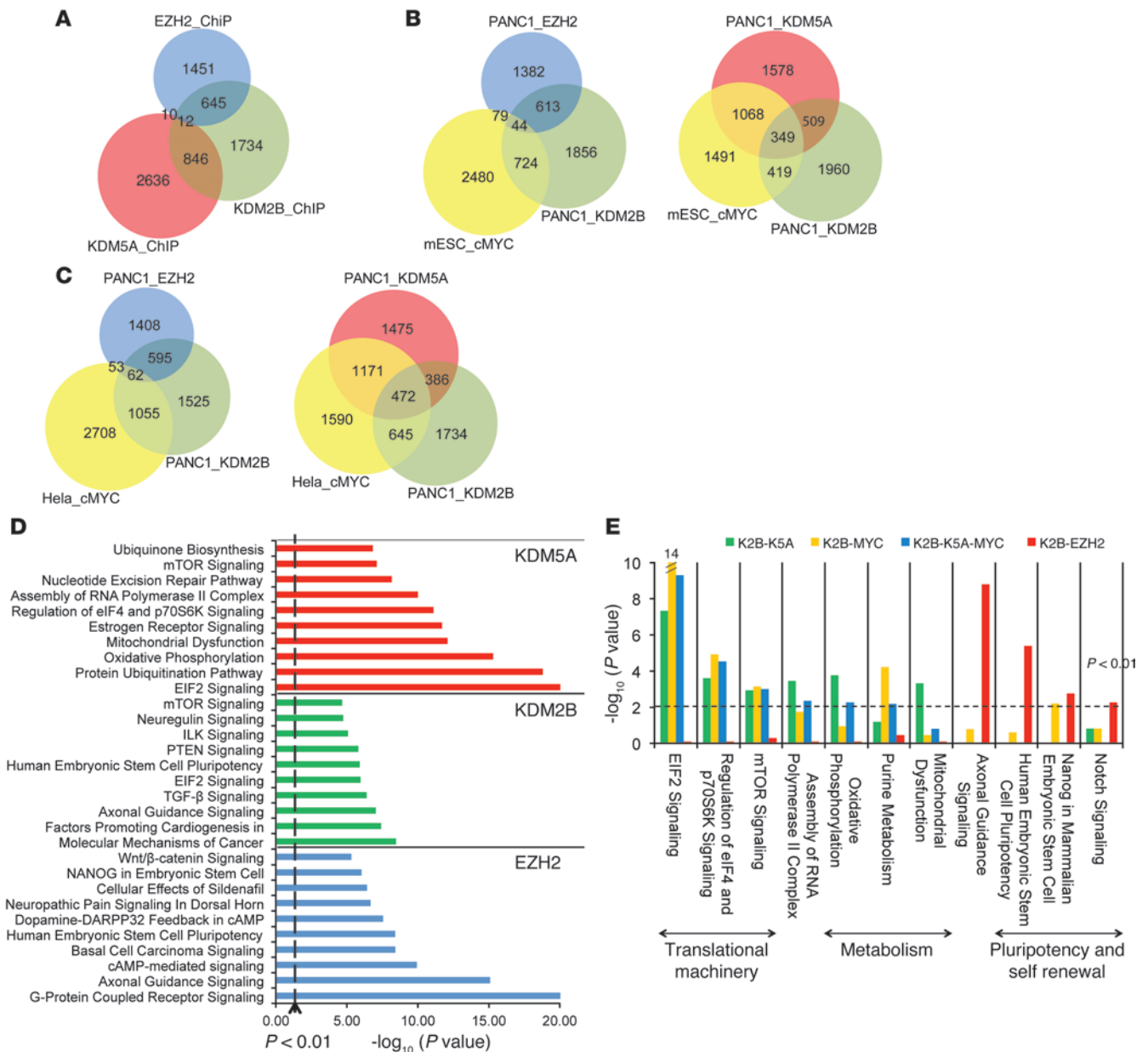


Figure 3
 KDM2B is required for Polycomb-mediated repression and for maintenance of a metabolic gene signature. **(A)** GSEA analysis of the KDM2B-dependent transcriptome in 6 PDAC cell lines. Shown are pathways that had the same direction of change in at least 5 of 6 lines. Gene sets with *P* values less than 0.05 were selected for comparison across the different cell lines. **(B)** IPA transcription factor prediction analysis to identify alterations in transcription factor activity induced by shKDM2B in PDAC cell lines (see Methods). Shown are transcription factors with *z* scores greater than 2 and *P* overlap values less than 0.01. **(C and D)** KDM2B knockdown downregulated expression of KDM5A transcript **(C)** and protein **(D)**. See also Supplemental Figure 3 and Supplemental Table 1.

particular, we found that KDM2B-EZH2-bound genes were largely inactive, whereas genes bound by KDM2B alone or in the context of MYC and/or KDM5A were enriched for H3K4me3 and actively transcribed (Figure 5D and Supplemental Figure 5B). In order to further relate chromatin binding to direct gene regulation, we integrated the KDM2B-dependent transcriptome (Figure 3) and ChIP-seq profiles in PANC1 cells. The data showed that 36% of the total set of genes bound by KDM2B were altered greater than 1.5-fold in response to KDM2B knockdown (22% upregulated, 14% downregulated; Figure 5, E and F). Strikingly, 34% of genes cobound by KDM2B-EZH2 were induced upon KDM2B knockdown (Figure 5, E and F), suggestive of a direct causal relationship between their transcriptional repression and KDM2B function. Conversely, approximately 10% of the KDM2B-EZH2-cobound genes were downregulated. The opposite pattern was seen for genes bound by KDM2B and KDM5A, where 18% were downregulated and only 7% were upregulated following knockdown of KDM2B (Figure 5, E and F); the predicted KDM2B-MYC targets showed a comparable pattern favoring reduced expression upon KDM2B knockdown

(Figure 5E). These findings demonstrated that interplay of KDM2B and EZH2 contributes to silencing of developmental programs in PDAC cells and revealed an unexpected function for KDM2B in the positive regulation of a cohort of genes controlling metabolic homeostasis that are cobound by KDM5A and/or MYC.

Differential roles of KDM2B in chromatin regulation at activated and repressed targets. We performed ChIP analysis of a series of candidate KDM2B targets identified by ChIP-seq in order to confirm that endogenous KDM2B cobound with EZH2 or with KDM5A-MYC at distinct sets of targets (Figure 6A). The PRC1 components BMI1 and RING1B also cobound to a subset of KDM2B-EZH2 targets (Supplemental Figure 6A and data not shown). Importantly, we verified that KDM2B knockdown upregulated the expression of development related genes cobound by EZH2 and downregulated the expression of genes involved in metabolic homeostasis cobound by MYC and/or KDM5A (Figure 6B). Consistent with functional interplay of different transcriptional modules, these KDM2B-EZH2-cobound targets were upregulated upon EZH2 knockdown in multiple cell lines (Figure 6C and Supplemental

**Figure 4**

KDM2B regulates 2 distinct transcriptional modules. **(A)** ChIP-seq results showing overlapping gene targets among KDM2B, EZH2, and KDM5A in PANC1 cells. **(B and C)** Overlap of KDM2B, EZH2, and KDM5A binding in PANC1 cells and of MYC binding in mouse ES cells **(B)** and HeLa cells **(C)**. **(D and E)** IPA of KDM2B, EZH2, and KDM5A target genes identified by Chip-seq, shown for each factor individually **(D)** and for the different KDM2B-cobinding modules **(E)**. The y axis (log scale) corresponds to the binomial raw P values. See also Supplemental Figure 4 and Supplemental Table 2.

Figure 6B), and those bound by KDM2B together with MYC and KDM5A showed decreased expression upon knockdown of either MYC or KDM5A (Figure 6C). Finally, whereas KDM2B cobound and interacted with PcG proteins at its target loci (present study and refs. 12, 36–38), we did not observe evidence for physical interactions between KDM2B and KDM5A or MYC (data not shown), which suggests that they bind common targets as components of independent complexes.

Subsequently, we examined the effect of KDM2B knockdown on the chromatin marks at these loci in PDAC cell lines. ChIP analysis of a series of KDM2B-EZH2 targets, including regula-

tors of pancreatic development such as *GATA6* and *JAG1*, showed that knockdown of KDM2B resulted in upregulated H3K36me2 and decreased H3K27me3, consistent with a loss of KDM2B and PRC2 activity, respectively, whereas no significant changes were observed in the levels of H3K4me3 (Figure 6D). Moreover, EZH2 and RING1B binding was reduced upon KDM2B knockdown (Figure 6D), which suggests that KDM2B may facilitate their targeting. Importantly, knockdown of KDM2B, EZH2, BMI1, or RING1B upregulated the expression of these cobound target genes in PDAC cell lines (Supplemental Figure 6C and data not shown). It is noteworthy that elevated expression of *GATA6*, which

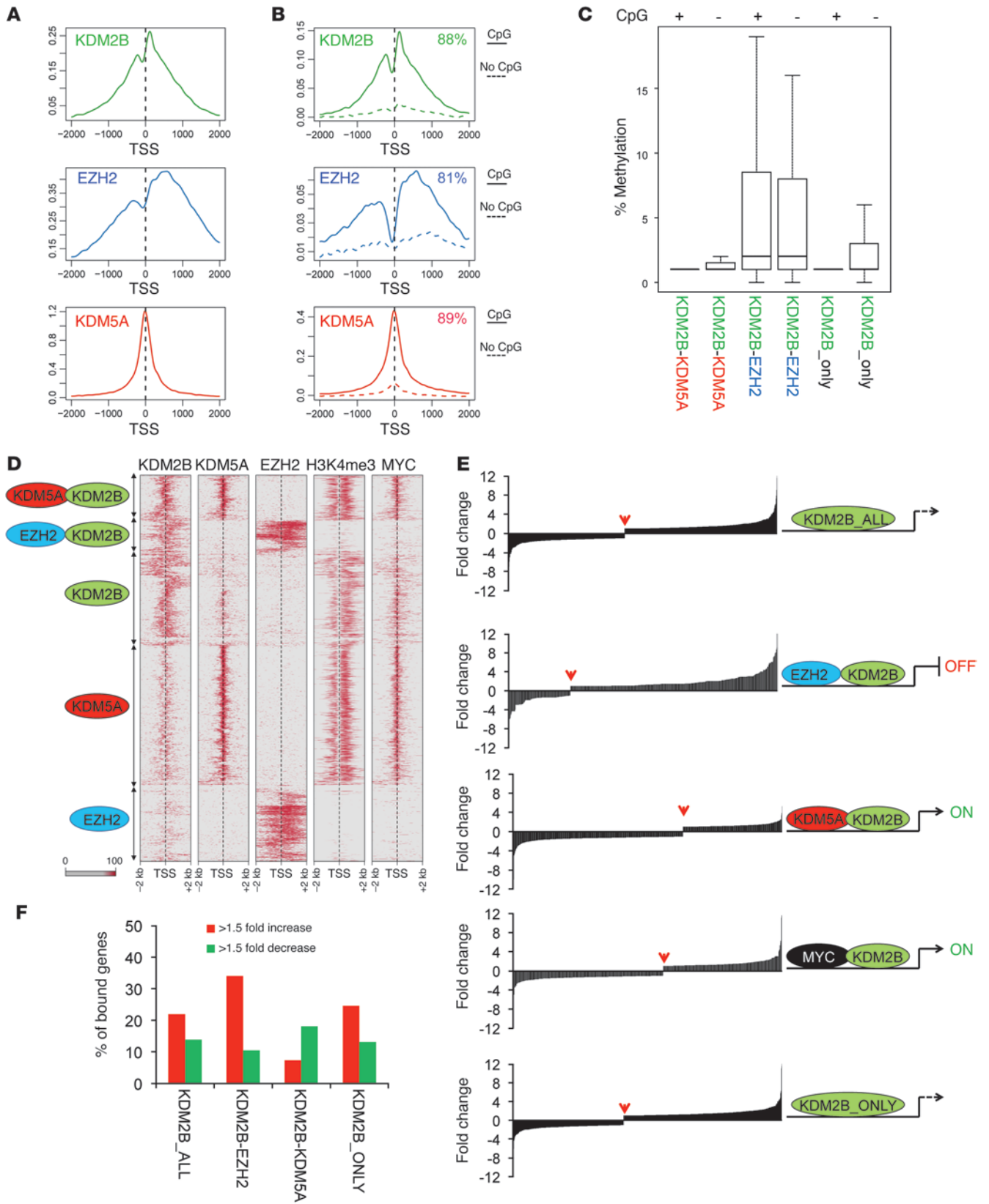




Figure 5

KDM2B negatively and positively regulates transcription through different modular associations. **(A)** Read density profiles of KDM2B, EZH2, and KDM5A around the TSS of bound genes. *x* axis, nucleotide coordinates around the TSS; *y* axis, average \log_2 ChIP-seq signal intensity. **(B)** Composite read density profiles of KDM2B, EZH2, and KDM5A binding in relation to the presence and absence of CpG islands around the TSS (axes as in **A**). The percentage of factor-bound genes that have CpG islands is shown. **(C)** Average percent methylation of cytosines in promoters of genes bound by different KDM2B modules in relation to the presence or absence of CpG islands, measured by reduced representation bisulfite sequencing. Boxes represent range between lower and upper quartiles; bands within boxes denote median; whiskers extend to the most extreme data point not more than 1.5 times the interquartile range; outliers are not shown. **(D)** Combinatorial binding profiles of KDM2B, EZH2, KDM5A, and H3K4me3 enrichment in PANC1 cells and MYC binding in HeLa cells. Each horizontal line represents a separate gene and its TSS. A ± 2 -kb window is shown for each gene. Bar shows average \log_2 ChIP-seq signal intensity. Binding profile overlap is shown at left. **(E and F)** Effect of KDM2B knockdown on expression of genes bound by KDM2B. **(E)** Effect of shKDM2B on expression of genes in different binding modules: total KDM2B-bound genes (KDM2B_ALL); cobinding with EZH2, KDM5A, or MYC; or none of these factors (KDM2B_ONLY). Downregulated and upregulated genes are plotted to the left and right, respectively, of the red arrows. KDM2B-EZH2-cobound genes were primarily upregulated, and those bound by KDM2B-KDM5A or KDM2B-MYC were downregulated. OFF, inactive; ON, active. **(F)** Graphical representation of data in **E** filtered for genes exhibiting greater than 1.5-fold difference in expression upon KDM2B knockdown. See also Supplemental Figure 5.

specifies the classical (epithelial) subtype of PDAC (4), exhibited an inverse correlation with KDM2B expression in both PDAC cell lines and human PDAC specimens (Supplemental Figure 6, D and E), supporting the relevance of this regulatory program. JAG1 showed a similar profile, with selective expression in classical PDAC lines and reactivation in quasimesenchymal lines upon KDM2B silencing (Supplemental Figure 6F). Thus, KDM2B acts in part to facilitate recruitment of PRC2 and PRC1, thereby silencing regulators of lineage specification in poorly differentiated PDAC cells. In contrast to the KDM2B-EZH2 targets, the set of genes activated by KDM2B had abundant H3K4me3, an epigenetic mark of active transcription, whereas KDM2B knockdown caused a robust decrease in H3K4me3 at these loci (Figure 6E and Supplemental Figure 6G), in line with the downregulation of these genes. These loci lacked H3K27me3 and either lacked or did not show consistent changes in H3K36me2 upon KDM2B knockdown (Figure 6E). Thus, the functions of KDM2B in the positive regulation of gene expression appear not to involve the demethylation of H3K36 or H3K4 at the target loci.

The gene targets positively regulated by KDM2B were highly enriched for loci encoding proteins involved in ribosomal and mitochondrial function (Figure 3B, Figure 4, D and E, and Supplemental Figure 4D), suggesting potential roles of KDM2B in energy homeostasis and global control of components of the translational machinery. Correspondingly, we observed that KDM2B knockdown induced AMPK, a key sensor of cellular energy status, as reflected by increased phosphorylation of AMPK α (T172) and reduced phosphorylation of ribosomal S6 protein (S235/236) (Supplemental Figure 6, E and F), the latter of which is consistent with AMPK-mediated inhibition of mTOR complex 1 (mTORC1). Comparable effects were observed upon knockdown of KDM5A

(Supplemental Figure 6, I and J). Notably, KDM2B knockdown sensitized PDAC cell lines to apoptosis under conditions of glucose deprivation (Figure 6F). Taken together, these data suggest that inactivation of the KDM2B-KDM5A-MYC transcriptional program induces an energy stress state in PDAC cells, which leads to cell death when nutrients are limiting.

Contributions of EZH2, MYC, and KDM2B to proliferation of poorly differentiated PDAC cell lines. To extend our data demonstrating the functional interplay between KDM2B and both PRC2 and KDM5A-MYC in the regulation of gene expression, we examined the roles of these factors in the growth of poorly differentiated PDAC cell lines. Importantly, knockdown experiments demonstrated that ablation of EZH2, MYC, and KDM5A led to pronounced decreases in the proliferation of multiple PDAC cell lines previously shown to be sensitive to KDM2B knockdown (Figure 7A). EZH2 and KDM5A responsiveness correlated with relative expression levels in these cell lines. Furthermore, overexpression of EZH2 partially rescued the proliferative arrest caused by KDM2B knockdown in MiaPaca cells (Figure 7B), whereas KDM5A did not rescue in this setting (data not shown), which suggests a prominent role for EZH2 as mediator of KDM2B-dependent effects on cell growth. Taken together, our results indicate that the capacity of KDM2B to sustain PDAC tumorigenicity involves dual roles in gene regulation: cooperation with PcG complexes silences cellular differentiation programs, and interplay with KDM5A and MYC activates metabolic and ribosomal gene expression (Figure 7C).

Discussion

In this study, we defined critical roles for KDM2B in PDAC pathogenesis and provided insights into the transcriptional functions of this chromatin-modifying enzyme. Examination of human tumor specimens coupled with genome-wide analyses revealed that KDM2B is a central driver of an epigenetic program critical for tumorigenicity of poorly differentiated (quasimesenchymal) PDAC. KDM2B is part of distinct transcriptional modules that have different functions in gene regulation: occupancy of TSSs together with PcG proteins suppresses lineage-specific genes, whereas cobinding with MYC and/or KDM5A positively regulates transcription of sets of genes involved broadly in metabolic homeostasis (Figure 7C). Loss of these transcriptional programs upon KDM2B silencing in PDAC cell lines resulted in upregulation of pancreatic differentiation genes, sensitization to apoptosis in response to energy stress, and pronounced reduction in tumorigenicity.

The important functional contributions of PcG proteins to KDM2B-regulated tumor maintenance that we defined in PDAC extend prior results demonstrating the interplay of KDM2B and EZH2 (11–13). By mapping the genome-wide chromatin binding sites of these enzymes and integrating the data with transcriptional changes caused by KDM2B modulation, we found that PRC2-mediated repression represents a major component of the KDM2B-regulated transcriptome, with 31% of EZH2 target genes cobound by KDM2B, and approximately 45% of these KDM2B-EZH2 targets showing differential expression (predominantly upregulation) upon KDM2B knockdown (Figure 5, E and F). KDM2B knockdown interfered with the binding of EZH2 — and of PRC1 components at certain loci, a function that correlates with H3K36me2 HDM activity. Given that PRC2 binding is inhibited by active chromatin marks, including di- and trimethylated H3K36 (39, 40), KDM2B may facilitate the recruitment of PRC2 to target loci through demethylation of H3K36. KDM2B also physically interacts with PcG proteins, both in mam-

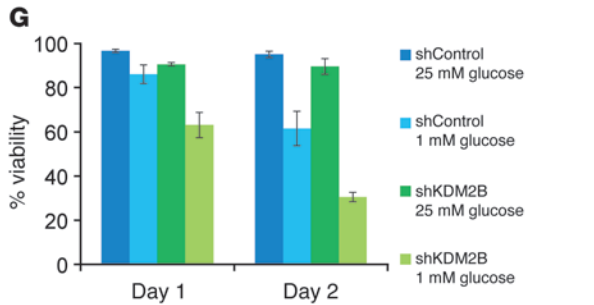
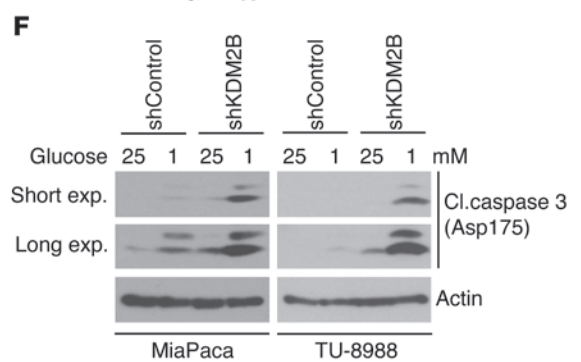
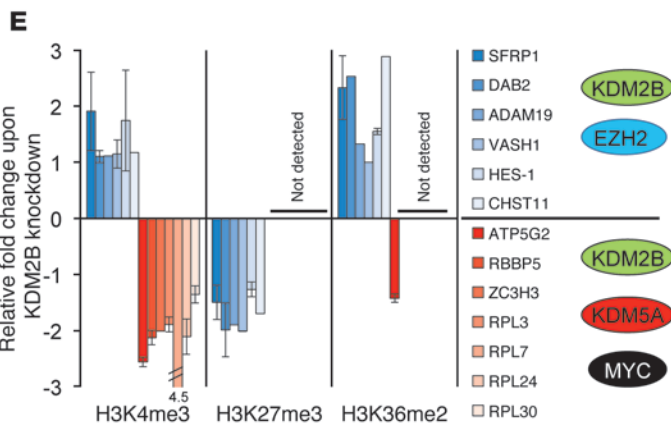
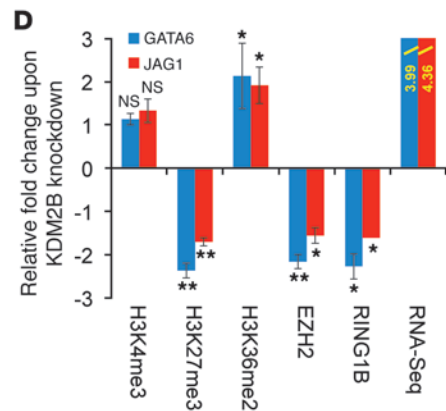
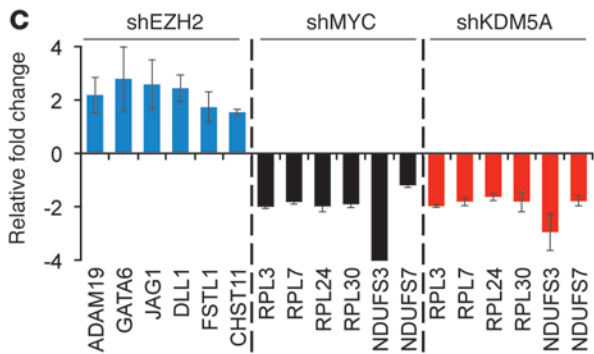
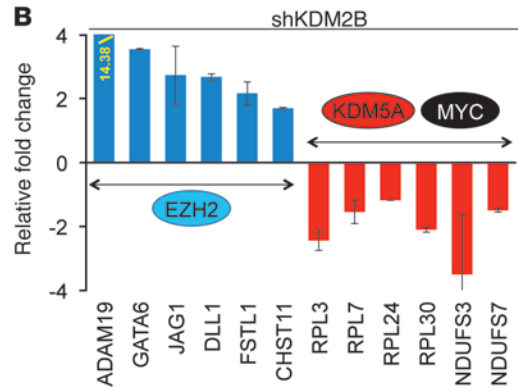
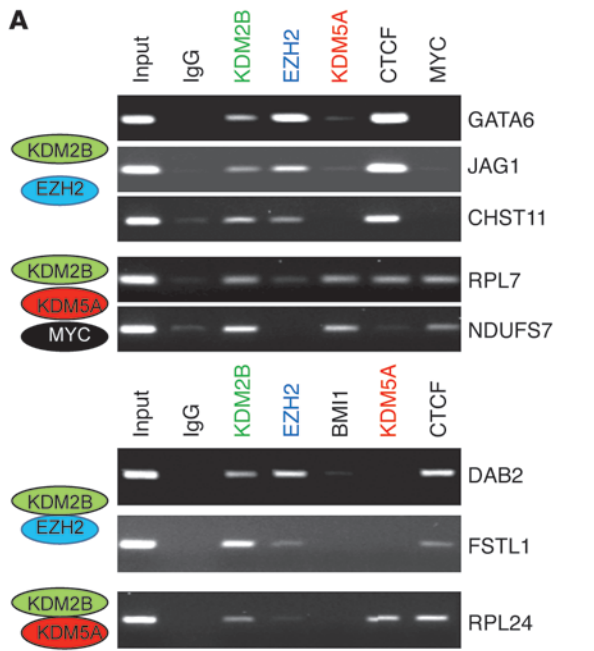




Figure 6

Differential roles of KDM2B in chromatin regulation at activated and repressed targets. (A) ChIP analysis of MiaPaca cells for binding of the indicated proteins to different KDM2B-EZH2 and KDM2B-KDM5A-MYC targets. (B and C) Quantitative RT-PCR analysis of expression changes of selected genes cobound by KDM2B-EZH2 or KDM2B-KDM5A-MYC in response to knockdown of (B) KDM2B or (C) EZH2, MYC, and KDM5A. Cobinding modules are represented by ovals. Note that genes cobound by KDM2B-EZH2 were upregulated upon KDM2B or EZH2 knockdown, whereas KDM2B-KDM5A-MYC-cobound genes were downregulated upon KDM2B, c-MYC, or KDM5A knockdown. (D) ChIP analysis showing the effect of KDM2B knockdown on the indicated histone marks and on binding of EZH2 and RING1B at selected KDM2B target genes in MiaPaca cells. Change in mRNA expression induced by KDM2B knockdown (RNA-seq) is also shown. Results are mean \pm SD. * $P < 0.05$; ** $P < 0.01$. (E) ChIP analysis showing relative fold enrichment of the indicated histone marks on selected target genes that define the different KDM2B modules in MiaPaca cells. KDM2B-EZH2-cobound and KDM2B-KDM5A-cobound genes are shown as blue and red bars, respectively. (F and G) The indicated PDAC cell lines were infected with shControl or shKDM2B lentiviruses and cultured for 36 hours in standard (25 mM) or reduced (1 mM) glucose concentrations. Attached and floating cells were analyzed (F) by Western blotting or (G) for viability (trypan blue dye exclusion method). See also Supplemental Figure 6 and Supplemental Table 3.

malian cells and in flies, which may contribute to the targeting of PRC1 and PRC2 (12, 36–38). Moreover, we observed that KDM2B positively regulated EZH2 levels in a subset of PDAC cell lines via epigenetic silencing of the *let-7b* and *miR-101* miRNAs, which target EZH2 (Supplemental Figure 7, A–C), as reported in other cell types (11, 13). Importantly, bioinformatic analysis of 2,158 human tumor specimens showed that the expression levels of EZH2 and KDM2B were closely correlated across tumor types (Supplemental Figure 7D) and in human PDAC specimens (Supplemental Figure 7E), and KDM2B showed the highest degree of coordinate regulation with EZH2 compared with all HDM family members (Supplemental Figure 7F). As silencing of PRC2 targets and induction of EZH2 are associated with poor differentiation and shortened survival across multiple cancer types, including PDAC (22, 27–30), these data establish the widespread importance of cooperation between KDM2B and PcG proteins in antagonizing developmental decisions in cancer.

Our ChIP-seq studies showed that greater than 25% of the KDM2B target loci were co-occupied by KDM5A in PDAC cells (Figure 4A). Likewise, integration of these data with publicly available datasets suggested that there was also considerable overlap in the binding of these 2 factors with c-MYC (Figure 4, B and C). This latter set of targets was greatly enriched for actively transcribed genes and genes that were downregulated upon KDM2B silencing (Figure 5, D–F). KDM2B did not appear to mediate demethylation of H3K36 or H3K4 at these loci; rather, KDM2B inactivation reduced H3K4me3 levels in accordance with the observed downregulation of gene expression. These observations implicate KDM2B in the positive regulation of transcription, which was unexpected based on prior functional studies. However, crosstalk between KDM2B and KDM5A is consistent with recent findings in *Drosophila* showing genetic interactions between dKDM2 and the KDM5A ortholog Lid (31). Moreover, while the best-characterized functions of KDM5A/Lid are in transcriptional repression through its H3K4 HDM activity, KDM5A/Lid has been shown to directly activate transcription by binding to MYC or to circadian transcription factors at target loci, a function independent of its

demethylase activity (31, 32, 41). In addition, published KDM5A genome-wide chromatin binding profiles in lymphoma and ES cells (35, 42, 43) show considerable overlap with our present observations in PDAC cells, connecting KDM5A to active transcription.

The set of genes positively regulated by KDM2B was highly enriched for components of the translational machinery and for mitochondrial function. These profiles are in line with the well-characterized role for MYC in metabolic regulation, including the requirement for induction of ribosomal genes for MYC oncogenic activity (44, 45). In addition, KDM5A has been shown to bind comparable sets of targets in multiple cell types and appears to be required for maintenance of mitochondrial function (35, 42, 43). While the magnitude of change in the expression of these KDM2B-KDM5A-MYC-bound genes upon KDM2B knockdown was less pronounced compared with the observed upregulation of the KDM2B-PcG targets, these profiles were remarkable in showing decreases in multiple components of key metabolic pathways (Figure 4E and Figure 6, B and C). KDM2B knockdown was associated with an energy stress response, as reflected by activation of AMPK signaling and downregulation of mTOR activity (Figure 4E, Figure 6, F and G, and Supplemental Figure 6, E–G). Moreover, these cells were highly sensitized to apoptosis upon energy depletion induced by glucose removal, which suggests that KDM2B maintains tumorigenesis by coordinating both metabolic and cell differentiation decisions (Figure 7C).

KDM5A is overexpressed in human PDAC specimens, and our data indicated that KDM2B contributes to this induction (Figure 3, C and D). Although further studies are needed to delineate the associated molecular mechanisms, it is noteworthy that *miR-101*, which is directly repressed by KDM2B (11, 13), is predicted to target KDM5A in addition to EZH2. KDM5A is also amplified in some PDAC specimens (2) and cell lines (e.g., TU-8902), and the c-MYC locus frequently shows copy number increases in these tumors (2, 46). Thus, genomic gains, upregulated expression, and functional synergy among these factors are together likely to contribute to the high activity of this transcriptional module in poorly differentiated PDAC.

Our observations linking KDM2B to the tumorigenicity of an aggressive subset of PDAC through integral roles in both PcG- and MYC-mediated transcriptional regulation are notable in light of the emerging relationship between cancers and pluripotent stem cells. Cancer cells and ES cells share the properties of indefinite self-renewal and blocked differentiation and have overlapping gene expression signatures, which supports the view that cancers are transcriptionally reprogrammed toward an ES cell-like state (22). Recent studies have suggested a refined model, showing that the ES cell self-renewal transcriptional program involves separate regulatory modules centering on PcG, MYC, and the core pluripotency factors (e.g., OCT4, KLF4, and NANOG); in cancers, the partial reactivation of this ES cell signature consisting of the PcG and MYC modules correlates with advanced stage and poor outcome (26). Thus, the dual transcriptional functions of KDM2B, involving PcG and MYC activity, that cooperate to drive the growth of poorly differentiated PDAC cells impinge directly on 2 distinct pluripotency networks. These findings, together with the previous demonstration that KDM2B enhances somatic cell reprogramming by OCT4 (15), are consistent with an ability of KDM2B to subvert differentiation in primary cells and to sustain undifferentiated states in advanced cancers.

In addition to predicting poor outcomes, the quasimesenchymal subtype of PDAC also appears to have signaling dependencies different from those of more epithelial (classical) tumors, as reflected

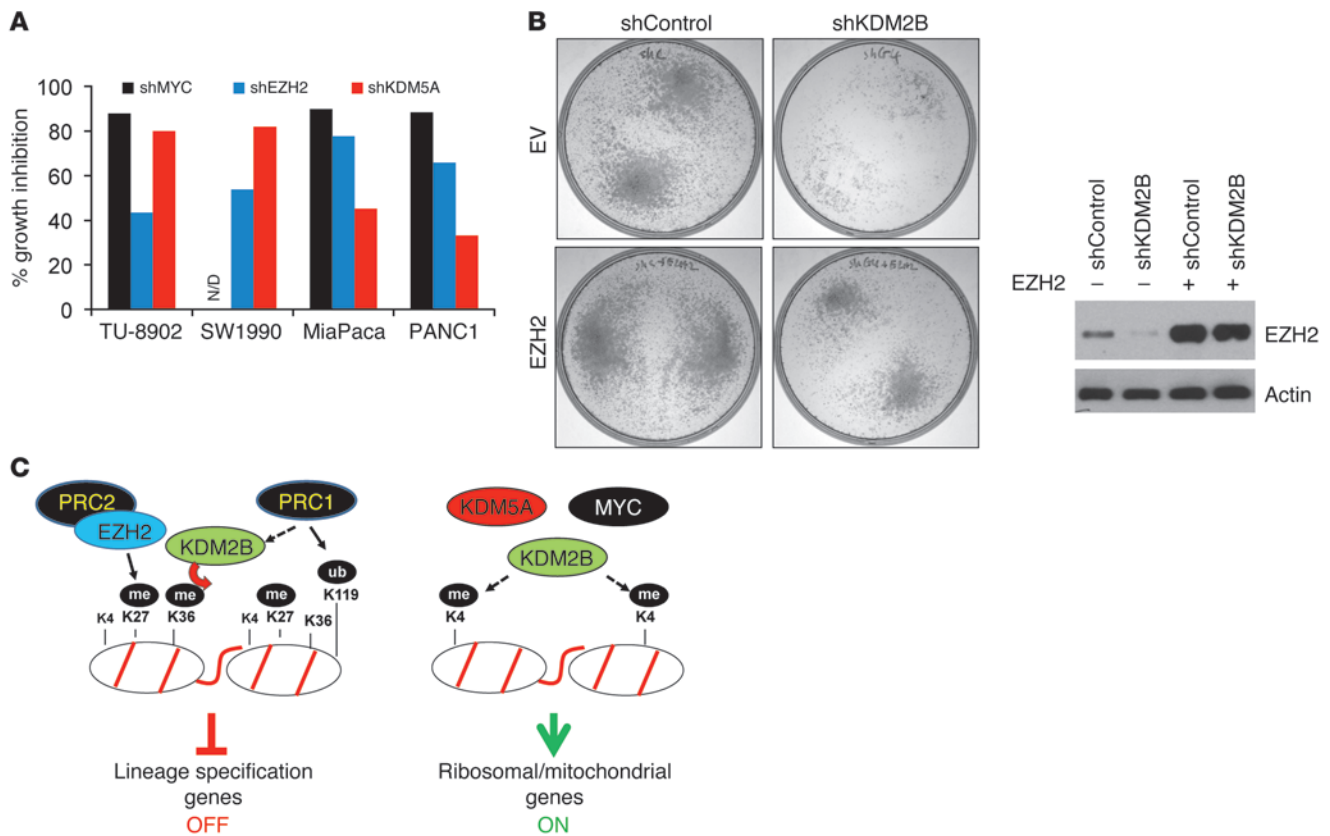


Figure 7

EZH2 mediates the proliferative effects of KDM2B in PDAC cell lines. **(A)** Percent growth inhibition of the indicated PDAC cell lines upon knockdown of c-MYC, EZH2, or KDM5A (at 9 days after seeding). N/D; not done. **(B)** 10^4 MiaPaca cells overexpressing EZH2 were infected with shKDM2B or shControl and plated on 6-cm plates. After 3 weeks, cells were stained and photographed. Efficient expression of EZH2 was demonstrated by Western blot. **(C)** KDM2B controls tumorigenicity via separate transcriptional repression and activation programs. KDM2B-PRC2 cobinding silences the expression of lineage specification genes (OFF) through H3K36 demethylation (red arrow) and H3K27 methylation (solid arrow) at the gene promoters. PRC1 participates in the silencing of a subset of these targets. KDM2B activates the expression of genes involved in metabolic homeostasis and protein synthesis (ON) in association with KDM5A and/or MYC. KDM2B does not regulate H3K36 or H3K27 methylation levels at these promoters, but rather is required to maintain the H3K4 mark of activated transcription (dashed arrows). me, methylation; ub, ubiquitination.

by previous studies in cell lines showing that the former subtype has reduced sensitivity to knockdown of the KRAS oncogene and altered responsiveness to anticancer drugs (3, 4). Our studies suggest that KDM2B regulates a critical epigenetic switch that balances developmental and metabolic decisions in these poorly differentiated PDAC cells. Since KDM2B catalytic activity appears to be required for tumorigenesis, small-molecule inhibitors may provide therapeutic benefit in this chemoresistant PDAC subtype.

Methods

Further information can be found in Supplemental Methods.

Xenograft experiments. Human PDAC cell suspensions were injected subcutaneously in the left (control) and right (KDM2B knockdown) flanks of SCID mice under sterile conditions using a 30-gauge needle and a 1-ml disposable syringe. The volume of inoculation was 100 μ l (5×10^5 tumor cells suspended in 100 μ l PBS). Mice were euthanized after 4–5 weeks, and tumors were excised, photographed and weighed.

Orthotopic injection and histological characterization. SCID mice (C3Sn.Smn.CB17-Prkdcscid/J, Jackson Lab) were subjected to general anesthesia with intraperitoneal Avertin (0.5 mg/g) and subcutaneous Marcaine (0.1 ml/25 g

mouse; 0.025% solution) analgesia, according to Massachusetts General Hospital Subcommittee on Research Animal Care guidelines. Orthotopic injections were performed as previously described (20). Briefly, a left lateral laparotomy was performed and spleen and distal pancreas were mobilized. 2×10^4 *Ptf1 α -Cre;LSL-Kras^{G12D}* cells (viability >90%) were suspended in 50 μ l pancreatic duct media, mixed with 50 μ l Matrigel (BD Biosciences), and injected into the pancreas. The abdominal incision was closed using silk suture 3/0 (Ethicon) for the peritoneum and surgical staples for the skin. After 4 weeks, mice were sacrificed, the whole pancreas was carefully sectioned with a surgical blade, and the longest nodule diameter was annotated. Experiments were conducted at least in triplicate for each condition. H&E slides were analyzed with an Olympus DP72 microscope.

Tumor histology and IHC scoring. We used a grading scheme endorsed by the WHO (47), which uses the combined assessment of glandular differentiation, mucin production, nuclear atypia, and mitotic activity (48). IHC was scored on a scale of 0–5, based on the percentage of tumor cells staining: 0, negative; 1, 0%–10%; 2, 11%–25%; 3, 26%–50%; 4, 51%–75%; 5, >76% (Figure 1H).

Statistics. Results are expressed as mean \pm SEM, unless otherwise specified. Significance was analyzed using 2-tailed Student’s *t* test. A *P* value less than 0.05 was considered statistical significant.



Study approval. All work with animals was conducted under protocol 2005N000148 approved by the Subcommittee on Research Animal Care, which serves as the IACUC for Massachusetts General Hospital. Experiments using human specimens were approved by the Office for the Protection of Research Subjects at the Dana Farber Cancer Institute and by the Partners Healthcare Institutional Review Board IRB. These studies were performed using discarded and deidentified human tissue and were deemed to have IRB exempt status not requiring informed consent.

Acknowledgments

We are grateful to Nick Dyson, Mo Motamedi, Leif Ellisen, and Rushika Perera for critical reading of the manuscript and to members of the Bardeesy lab for helpful discussions throughout the course of these studies. This work was supported by grants from the

Waxman Foundation, the NCI (P01 CA117969-06, P50 CA127003, and 1 R01 CA133557-01), the Andrew Warshaw Institute, and the Lynda J. Verville Foundation to N. Bardeesy. A. Tzatsos is supported by the Nestora fund, NIH grant K99 CA158582, and the Massachusetts Biomedical Research Corporation Tosteson Fellowship Award.

Received for publication April 30, 2012, and accepted in revised form November 26, 2012.

Address correspondence to: Alexandros Tzatsos or Nabeel Bardeesy, 185 Cambridge Street, Boston, Massachusetts 02114, USA. Phone: 617.643.3156; Fax: 617.643.3170; E-mail: Tzatsos.Alexandros@mgh.harvard.edu (A. Tzatsos). Phone: 617.643.2579; Fax: 617.643.3170; E-mail: Bardeesy.Nabeel@mgh.harvard.edu (N. Bardeesy).

- Hidalgo M. Pancreatic cancer. *N Engl J Med*. 2010; 362(17):1605–1617.
- Jones S, et al. Core signaling pathways in human pancreatic cancers revealed by global genomic analyses. *Science*. 2008;321(5897):1801–1806.
- Singh A, et al. A gene expression signature associated with “K-Ras addiction” reveals regulators of EMT and tumor cell survival. *Cancer Cell*. 2009; 15(6):489–500.
- Collisson EA, et al. Subtypes of pancreatic ductal adenocarcinoma and their differing responses to therapy. *Nat Med*. 2011;17(4):500–503.
- Rodriguez-Paredes M, Esteller M. Cancer epigenetics reaches mainstream oncology. *Nat Med*. 2011;17(3):330–339.
- Chi P, Allis CD, Wang GG. Covalent histone modifications—miswritten, misinterpreted and mis-erased in human cancers. *Nat Rev Cancer*. 2010; 10(7):457–469.
- Kampranis SC, Tschlis PN. Histone demethylases and cancer. *Adv Cancer Res*. 2009;102:103–169.
- van Haaften G, et al. Somatic mutations of the histone H3K27 demethylase gene UTX in human cancer. *Nat Genet*. 2009;41(5):521–523.
- Rui L, et al. Cooperative epigenetic modulation by cancer amplicon genes. *Cancer Cell*. 2010;18(6):590–605.
- Pfau R, Tzatsos A, Kampranis SC, Serebrennikova OB, Bear SE, Tschlis PN. Members of a family of JmjC domain-containing oncoproteins immortalize embryonic fibroblasts via a JmjC domain-dependent process. *Proc Natl Acad Sci U S A*. 2008; 105(6):1907–1912.
- Kottakis F, Polytaichou C, Foltopoulou P, Sanidas I, Kampranis SC, Tschlis PN. FGF-2 regulates cell proliferation, migration, and angiogenesis through an NDY1/KDM2B-miR-101-EZH2 pathway. *Mol Cell*. 2011;43(2):285–298.
- Tzatsos A, Pfau R, Kampranis SC, Tschlis PN. Ndy1/KDM2B immortalizes mouse embryonic fibroblasts by repressing the Ink4a/Arf locus. *Proc Natl Acad Sci U S A*. 2009;106(8):2641–2646.
- Tzatsos A, et al. Lysine-specific demethylase 2B (KDM2B)-let-7-enhancer of zester homolog 2 (EZH2) pathway regulates cell cycle progression and senescence in primary cells. *J Biol Chem*. 2011; 286(38):33061–33069.
- He J, Kallin EM, Tsukada Y, Zhang Y. The H3K36 demethylase Jhdml1b/Kdm2b regulates cell proliferation and senescence through p15(Ink4b). *Nat Struct Mol Biol*. 2008;15(11):1169–1175.
- Wang T, et al. The histone demethylases Jhdml1a/1b enhance somatic cell reprogramming in a vitamin-C-dependent manner. *Cell Stem Cell*. 2011; 9(6):575–587.
- He J, Nguyen AT, Zhang Y. KDM2B/JHDM1b, an H3K36me2-specific demethylase, is required for initiation and maintenance of acute myeloid leukemia. *Blood*. 2011;117(14):3869–3880.
- Maitra A, Hruban RH. Pancreatic cancer. *Annu Rev Pathol*. 2008;3:157–188.
- Aguirre AJ, et al. Activated Kras and Ink4a/Arf deficiency cooperate to produce metastatic pancreatic ductal adenocarcinoma. *Genes Dev*. 2003; 17(24):3112–3126.
- Hingorani SR, et al. Preinvasive and invasive ductal pancreatic cancer and its early detection in the mouse. *Cancer Cell*. 2003;4(6):437–450.
- Corcoran RB, et al. STAT3 plays a critical role in KRAS-induced pancreatic tumorigenesis. *Cancer Res*. 2011;71(14):5020–5029.
- Bardeesy N, et al. Both p16(Ink4a) and the p19(Arf)-p53 pathway constrain progression of pancreatic adenocarcinoma in the mouse. *Proc Natl Acad Sci U S A*. 2006;103(15):5947–5952.
- Ben-Porath I, et al. An embryonic stem cell-like gene expression signature in poorly differentiated aggressive human tumors. *Nat Genet*. 2008; 40(5):499–507.
- Kondo Y, et al. Gene silencing in cancer by histone H3 lysine 27 trimethylation independent of promoter DNA methylation. *Nat Genet*. 2008; 40(6):741–750.
- Wilson BG, et al. Epigenetic antagonism between polycomb and SWI/SNF complexes during oncogenic transformation. *Cancer Cell*. 2010;18(4):316–328.
- Shain AH, et al. Convergent structural alterations define SWI/SNF/Sucrose NonFermentable (SWI/SNF) chromatin remodeler as a central tumor suppressive complex in pancreatic cancer. *Proc Natl Acad Sci U S A*. 2012;109(5):E252–E259.
- Kim J, et al. A Myc network accounts for similarities between embryonic stem and cancer cell transcription programs. *Cell*. 2010;143(2):313–324.
- Ougolkov AV, Bilim VN, Billadeau DD. Regulation of pancreatic tumor cell proliferation and chemoresistance by the histone methyltransferase enhancer of zeste homolog 2. *Clin Cancer Res*. 2008; 14(21):6790–6796.
- Toll AD, et al. Implications of enhancer of zeste homolog 2 expression in pancreatic ductal adenocarcinoma. *Hum Pathol*. 2010;41(9):1205–1209.
- Kleer CG, et al. EZH2 is a marker of aggressive breast cancer and promotes neoplastic transformation of breast epithelial cells. *Proc Natl Acad Sci U S A*. 2003;100(20):11606–11611.
- Yu J, et al. A polycomb repression signature in metastatic prostate cancer predicts cancer outcome. *Cancer Res*. 2007;67(22):10657–10663.
- Li L, Greer C, Eisenman RN, Secombe J. Essential functions of the histone demethylase lid. *PLoS Genet*. 2010;6(11):e1001221.
- Secombe J, Li L, Carlos L, Eisenman RN. The Trithorax group protein Lid is a trimethyl histone H3K4 demethylase required for dMyc-induced cell growth. *Genes Dev*. 2007;21(5):537–551.
- Sharma SV, et al. A chromatin-mediated reversible drug-tolerant state in cancer cell subpopulations. *Cell*. 2010;141(1):69–80.
- Lin W, et al. Loss of the retinoblastoma binding protein 2 (RBP2) histone demethylase suppresses tumorigenesis in mice lacking Rb1 or Men1. *Proc Natl Acad Sci U S A*. 2011;108(33):13379–13386.
- Ram O, et al. Combinatorial patterning of chromatin regulators uncovered by genome-wide location analysis in human cells. *Cell*. 2011;147(7):1628–1639.
- Sanchez C, Sanchez I, Demmers JA, Rodriguez P, Strouboulis J, Vidal M. Proteomics analysis of Ring1B/Rnf2 interactors identifies a novel complex with the Fbxl10/Jhdml1B histone demethylase and the Bcl1 interacting corepressor. *Mol Cell Proteomics*. 2007;6(5):820–834.
- Gearhart MD, Corcoran CM, Wamstad JA, Bardwell VJ. Polycomb group and SCF ubiquitin ligases are found in a novel BCOR complex that is recruited to BCL6 targets. *Mol Cell Biol*. 2006;26(18):6880–6889.
- Lagarou A, et al. dKDM2 couples histone H2A ubiquitylation to histone H3 demethylation during Polycomb group silencing. *Genes Dev*. 2008; 22(20):2799–2810.
- Yuan W, Xu M, Huang C, Liu N, Chen S, Zhu B. H3K36 methylation antagonizes PRC2-mediated H3K27 methylation. *J Biol Chem*. 2011; 286(10):7983–7989.
- Schmitges FW, et al. Histone methylation by PRC2 is inhibited by active chromatin marks. *Mol Cell*. 2011; 42(3):330–341.
- DiTacchio L, et al. Histone lysine demethylase JARID1a activates CLOCK-BMAL1 and influences the circadian clock. *Science*. 2011;333(6051):1881–1885.
- Lopez-Bigas N, et al. Genome-wide analysis of the H3K4 histone demethylase RBP2 reveals a transcriptional program controlling differentiation. *Mol Cell*. 2008;31(4):520–530.
- Peng JC, et al. Jarid2/Jumonji coordinates control of PRC2 enzymatic activity and target gene occupancy in pluripotent cells. *Cell*. 2009; 139(7):1290–1302.
- Grewal SS, Li L, Orian A, Eisenman RN, Edgar BA. Myc-dependent regulation of ribosomal RNA synthesis during Drosophila development. *Nat Cell Biol*. 2005;7(3):295–302.
- Arabi A, et al. c-Myc associates with ribosomal DNA and activates RNA polymerase I transcription. *Nat Cell Biol*. 2005;7(3):303–310.
- Birnbaum DJ, et al. Genome profiling of pancreatic adenocarcinoma. *Genes Chromosomes Cancer*. 2011; 50(6):456–465.
- Hamilton SR, Aaltonen LA, eds. *Pathology and genetics of tumours of the digestive system*. Lyon, France: IARC Press; 2000.
- Hruban RH, et al. Pancreatic intraepithelial neoplasia: a new nomenclature and classification system for pancreatic duct lesions. *Am J Surg Pathol*. 2001; 25(5):579–586.